



# Experimental and Numerical Modeling of Bearing Capacity of Foundations on Soft Clay Stabilized with Granular Material

Zahra Bashir Malik<sup>1</sup> · Badee Alshameri<sup>1</sup> · Syed Muhammad Jamil<sup>1</sup> · Daanyal Umar<sup>1</sup>

Received: 17 August 2021 / Accepted: 1 November 2021 / Published online: 13 November 2021  
© The Author(s), under exclusive licence to Springer Nature Switzerland AG 2021

## Abstract

Over-excavation and replacement are the most commonly used ground modification techniques for shallow foundations. In soft soils, however, the extent of replacement by relatively larger (up to 19 mm) granular material was unknown. A total of 97 tests, consisting of 10 small and 87 numerical model tests, were carried out on two types of foundations, namely strip, and square. The width  $W$  and the depth of the replaced zone  $H$  were varied in each test and the ultimate bearing capacity  $q_u$  was calculated. The experimental and numerical analyses were compared by computing  $q_u$  from two methods (tangent intersection method (TIM) and  $0.1B$  method). The improvement in  $q_u$  was plotted as the dimensionless factor bearing capacity ratio (BCR) vs. depth ratio  $H/B$  for each foundation. A significant increase in BCR was observed from  $H/B$  of 1.5 to 4 for strip foundation and 2.5 to 3 for a square foundation. There was an insignificant increase in BCR after  $H/B$  of 4 and 3 for strip and square foundations, respectively. The width of the replacement was recommended as  $2B$  for square foundations, while no value was suggested for strip foundation owing to a steady increase in the BCR. In addition, it has been observed that the depth of replacement is a major component in improving the bearing capacity compared to the width of replacement.

**Keywords** Bearing capacity · Small-scale test · Finite element analysis · Soft clay · Granular replacement

## Introduction

The increased need for development activities in urban areas requires good construction sites. The accessible sites with problematic geomaterials have always been a challenge for geotechnical engineers and methods of expanding the use of these sites have become a priority. These methods have been identified as *ground modification techniques*. One of the oldest, simplest, and most widely used technique for ground modification of shallow foundations is *over-excavation and replacement* [1]. This method removes weak soil

and replaces it with a stronger one to increase its bearing capacity, reduce settlement, prevent expansion/contraction or freeze–thaw. No special equipment or labor is required for the replacement process. The replacement can be complete or partial, but a partial replacement is preferred due to its cost-effectiveness. The partial replacement is only effective if the structure's performance is not affected by it [2].

The dimensioning of an over-excavated and replaced section of soil requires the replaced area to be larger than the area of the foundation. The width of the replaced zone must range from  $B$  to  $3B$  (where  $B$  = width of the foundation), while the depth of the replaced zone must be between  $0.5B$  and  $1.5B$ . The minimum thickness of the replaced zone was suggested to be 500 mm [1]. There are four probable failure cases for foundations with the replaced zone, described as (i) general shear failure within a replaced zone, (ii) punching shear failure through the replaced zone, (iii) distributed failure through the replaced zone, and (iv) punching shear failure of a replaced zone [2].

The analysis using theoretical approaches [3–5] and large-scale field tests [6–9] have been carried out by various researchers to analyze the foundations resting

✉ Badee Alshameri  
badee.alshameri@yahoo.com; b.alshameri@nice.nust.edu.pk

Zahra Bashir Malik  
zahrabmalik@yahoo.com;  
zmalik.ms16nice@student.nust.edu.pk

Syed Muhammad Jamil  
dean@scee.nust.edu.pk

Daanyal Umar  
daanyal.ms16@nice.nust.edu.pk

<sup>1</sup> National University of Sciences and Technology,  
Islamabad 44000, Pakistan

on problematic geomaterial that has been replaced by a granular trench. The large-scale field tests were not recommended in comparison to the small-scale tests due to their high implementation effort or cost.

The small-scale test programs on soft clay were mostly carried out using sand as a replacement material. The improvement of the bearing capacity was investigated for strip foundations by varying the depth ratio— $H/B$  (depth of replacement to the width of foundation) from 0 to 4. Up to a depth ratio of 2.5 to 3, the impact of the replacement was validated to be significant, after a  $H/B$  of 3 the effect was insignificant [10]. The improvement effect was prominent till the depth ratio of 4, with the recommended value of granular thickness observed to be  $3B$  [11]. From the theoretical analysis of strip foundations in weak soil stabilized with granular material, it was found that the peak improvement occurs when the depth ratio is between 2.75 and 3.25 [3]. While the recommended trench thickness was  $1.5B$  for sand stabilized soft clay, no significant increase was observed after  $1.5B$ . The increase in  $q_u$  by the replacement depends mainly on two parameters, namely the undrained shear strength ( $s_u$ ) and the angle of internal friction ( $\varphi$ ) [12]. It has been observed that the improvement in  $q_u$  is mainly influenced by  $\varphi$ , rather than the width of the replaced zone [4], while the size and shape of the foundation did not affect in  $q_u$  rise [13]. While using sand as a replacement material in problematic clay, only a 7% increase in  $q_u$  was observed when using  $0.1B$  and tangent intersection methods [14].

When using Reclaimed Asphalt Pavement (RAP) as a replacement material in soft clay, the maximum benefit of the strip foundation was achieved with the width and depth of the replacement of  $2B$  and  $1B$ , respectively. For the square foundation, a maximum increase in  $q_u$  was observed at  $1.6B$  and  $0.6B$  width and depth of the replacement. In addition, it has been found that the improvement in  $q_u$  of such a system is mainly based on the width of the replaced zone, rather than its depth [15]. When Geogrid Micro-Mesh (GMM) in soft clay was used to stabilize strip foundations, a significant improvement was observed at a depth ratio of 2, and a clear failure point was observed at  $H/B = 3$ . These results were obtained by applying a pressure greater than 85 kPa [16]. Using stone as a replaced material in a weak clay and reducing the water content, an overall increase of 15% occurred in  $q_u$ . For a square foundation, the maximum strength was achieved with an equivalent width of replacement of  $2B$  and a depth ratio of 1.5. In this study, it was also found that the shape of a replaced zone also affects the stabilization of the clay matrix. The trench-shaped replaced zone showed 20% higher improvement values compared to square one [17].

The finite element methods (FEM) have become popular among engineers for modeling construction works. Several user-friendly softwares have been developed for modeling

the soil strength and deformation behaviour of soft soils [18]. However, there are some problems with predicting the strength and deformation behaviour of soft soils. Numerical analysis is influenced by various factors such as simplified geometry and boundary conditions, mesh generation, initial ground conditions, and the type of relationship chosen to model soil behaviour. For a good prediction of results, the parameters, the simulation method [19], and the construction process [20] must be carefully adopted.

The studies on improving the bearing capacity using well-graded sand compared to poorly graded sand have been carried out by various authors [21–25]. The results were also validated with finite element modeling softwares, and PLAXIS 2D was used for this purpose in some studies [12, 22, 25, 26]. The three-point Gaussian integration rule was used for calculating the element stiffness matrices for strip foundation on dense sand layer underlain by soft clay [12]. The isotropic hardening model was used with Mohr–Coulomb failure criteria, and a triangular trench was constructed because of the construction difficulties of a rectangular trench in loose sand [22]. The stabilization of loose sand was carried out with dense sand and geosynthetics as reinforcement for the trench. It was found that the application of geosynthetics and increased density of the trench material improved the load-carrying capacity. A good comparison between theoretical and experimental results was also found for the non-linear soil hardening model [25]. Axisymmetric and Mohr–Coulomb models were used in evaluating the circular foundation. The boundary effect was eliminated by taking the horizontal and vertical boundaries at  $5D$  and  $4D$ , respectively. The optimum value of the fill thickness to improve the bearing capacity was found at  $0.8D$ . Although no optimum value for fill length was recommended because the confinement of failure surface is limited within granular fill [26]. The SIGMA/W program was used to determine the scale effect of replacement and it has been found that the maximum improvement occurs when the depth ratio is 2 and the width of replacement is  $0.75B$  [27]. The numerical analysis using the finite difference approach was performed with FLAC3D and it was analyzed that replacing weak soil with granular material increases bearing pressure by approximately 80%. The maximum improvement was achieved with  $H/B$  of 5 [28]. The lower bound finite element analysis carried out in FLAC 2D showed a direct relationship between the bearing capacity and width, depth, and  $\varphi$  of the replaced material [29, 30]. For sands with small  $\varphi$  over larger  $c_u/\gamma B$ , the relationship was found to be complex. By increasing the depth ratio in such soils, the bearing capacity initially decreased and then began to increase [23]. However, a direct relationship was found between the bearing capacity with  $\varphi$  and  $q/\gamma B$  [1].

In previous studies, sand, reclaimed asphalt pavement, or GMM were used as replacement materials, as cited in

Table 1. In the present study, the granular material with a maximum particle size of 19 mm was used as replacement material on soft clay. This material is considered to be the most widely used soft soil improvement material in Pakistan due to its abundance. During this study, the small-scale tests were conducted on two types of foundations, namely strip and square. The extent of the replacement was examined by varying the width of the replacements from  $B$  to  $3B$  and the depth of the replacements from  $B$

to  $5B$ . The effect of the improvement was determined in terms of an improvement in the ultimate bearing capacity. The analysis was validated and compared in the finite element modeling program PLAXIS 2D V8. The width of replacement and depth ratio was recommended for both types of foundations.

**Table 1** Summary of existing methods

Researcher	Analysis type	Soil type	Replaced material	Width of replaced material	Thickness of replaced material
<b>Strip foundation</b>					
[3]	Theoretical analysis (upper bound theorem)	Soft clay	Granular material	–	$2.75B$ – $3.25B$
[10]	Small-scale testing	SP-sea sand	SP-river sand	–	$2.5B$ – $3B$
[11]	Small-scale testing	CL	Sand	–	$3B$
[12]	Small-scale testing + PLAXIS	CH	SP-Mumbra sand and geosynthetic reinf	–	$1.5B$
[61]	Small-scale testing	SP	SW + Geogrid	–	$2B$ (23% increase)
[13]	Small-scale testing	CL	SP	–	$0.8B$
[27]	SIGMA/W	Red clay	Ottawa sand + geogrid	$0.75B$	$2B$
[21]	Small-scale testing + PLAXIS 2D	SP-sea sand	SP-river sand	–	$1.4B$
[16]	Small-scale testing	CH	SP + GMM	–	$2B$ – $3B$
[15]	Small-scale testing	CL	RAP (reclaimed asphalt pavement)	$2B$	$B$
[30]	Lower bound finite element analysis	Soft clay	Granular material	$2B$	$4B$ – $5B$ (dense sand) $3.2B$ – $4B$ (med. sand)
[29]	FLAC 2D	Clay	Granular material	–	$5B$
<b>Square Foundation</b>					
[13]	Small-scale testing	CL	SP and geotextile reinf	–	$0.6B$
[15]	Small scale testing	CL	RAP (reclaimed asphalt pavement)	$1.6B$	$0.6B$
[17]	Small scale testing	CL	Stone	$2B$	$1.5B$
<b>Circular foundation</b>					
[13]	Small-scale testing	CL	SP and geotextile reinf	–	$0.6B$
[8]	Large-scale tests + PLAXIS 2D V8.6	CH	GW-GM	–	$1B^*$
[51]	Large-scale testing + ANN and MLR	CH	GW-GM	–	$2B^*$
[7]	Large-scale testing	Soft clay	Granular fill and geogrid reinforced granular fill	–	$0.75B^*$
[60]	PLAXIS 2D	Soft clay	Medium to loose sand (series 1) and very dense sand (series 2)	$2B$	$2B$ – $4B$ (placed at surface) $4B$ – $6B$ (placed at depth = $B$ )
[26]	PLAXIS 2D	Clay	GW-GM	–	$0.8B^*$
[30]	FEM analysis	Soft clay	Granular	$5B$	$1B^*$
<b>Rectangular foundation</b>					
[13]	Small-scale testing	CL	SP-sand and geotextile reinf	–	$0.8B$
[14]	Small-scale testing	CL-silty clay soil	SP and reinforcement layer	–	$0.6B$ (7% increase)

$B^*$  = diameter of foundation

## Small-scale Testing

### Materials

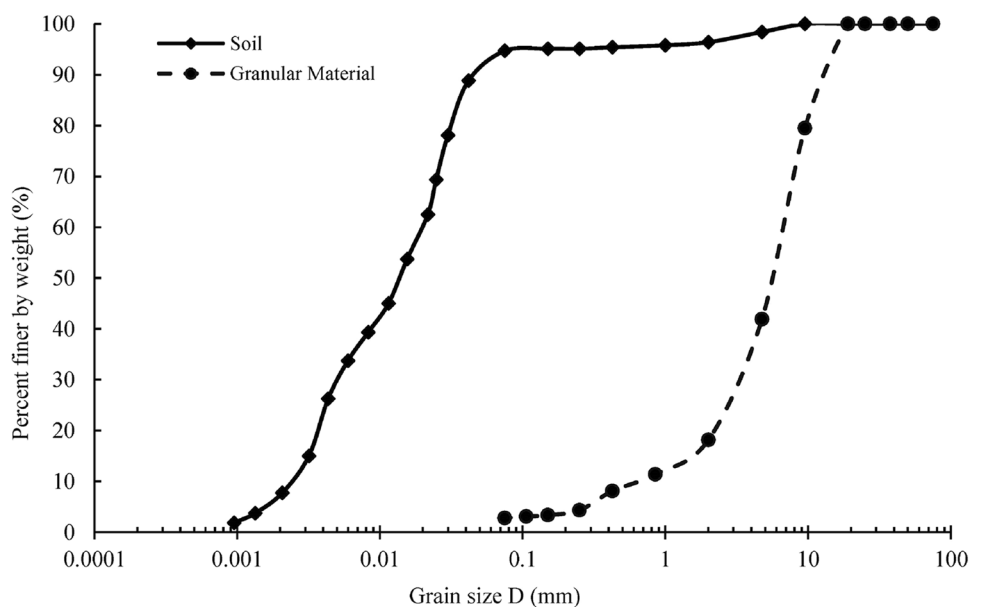
Two materials were used for small-scale modeling in the laboratory, i.e., low strength soil and granular material. The soil was taken from Dandi Gujran, Rawalpindi, Pakistan, which is located 11 km away from Chakri Interchange as shown in Fig. 1. The latitude (LAT) and Longitude (LONG) of the area were 33°13'45.2"N and 72°41'40.6"E, respectively. The natural moisture content ( $w$ ) was observed to

be 17.67% [31]. The specific gravity of soil solids ( $G_s$ ) was found to be 2.696 [32]. Particle-size distribution [33] showed the percentage of gravels as 1.6%, sand 3.7%, and fines as 94.7%. Hydrometer analysis [34] found the clay size particles to be 30% as shown in Fig. 2. The liquid limit (LL) was obtained as 42.04% and the plastic limit (PL) as 22.74% [35]. The soil was found to have a medium swelling potential [36], and it was classified as CL—Lean Clay described as reddish-brown low plasticity clay [37]. The moisture–unit weight relationship found that  $\gamma_{d,max}$  was 16.9 kN/m<sup>3</sup> at an OMC of 15% [31]. The relationship between the Liquidity Index (LI) and Undrained Shear Strength ( $s_u$ ) was produced



Fig. 1 Location of material collection areas

Fig. 2 Particle size distribution curves of soil and granular material





[32] by leaving the samples standing for 4 days (96 h). The graph was drawn between LI and  $\log_{10} s_u$  and an exponential line was taken as the best fit line [33]. The clay was categorized as soft clay when its undrained shear strength was between 12.5 and 25 kPa [34]. For this range of  $s_u$ , the liquidity index of 0.27–0.5 was required in the soil, taken from Fig. 3. The moisture content is calculated using Fig. 4, and it was found that  $w$  must be within 27.7–32.8% (approximately 28–33%) for the range of LI. In the case of small-scale modeling, the soil must have to be in a looser condition than in the full-scale test condition [35]. Therefore, in the present study, the undrained shear strength for carrying out the small-scale tests was assumed to be 13 kPa, with an LI of 0.50. To achieve this strength, dry unit weight of

14.31 kN/m<sup>3</sup> with a water content of 32% was required, as shown in Fig. 4. To validate the modulus of elasticity and cohesion, a triaxial test was carried out on the soil sample [36], in which the sample was prepared and left for 24 h before compaction. The results showed a good agreement, as the cohesion was obtained as 21.8 kPa at a dry density of 15.2 kN/m<sup>3</sup>. The permeability of soft clay was determined to be  $1.009 \times 10^{-9}$  m/s [37].

The granular material was collected from Haripur, Khyber Pakhtunkhwa, Pakistan, from the downstream side of the Khanpur Dam spillway with a maximum particle size of 19 mm. The latitude (LAT) and Longitude (LONG) of the area were 33°47'38.5"N and 72°54'13.5"E, respectively, as shown in Fig. 1. The gradation of the soil found

**Fig. 3** Plot of LI vs. undrained shear strength (kPa)

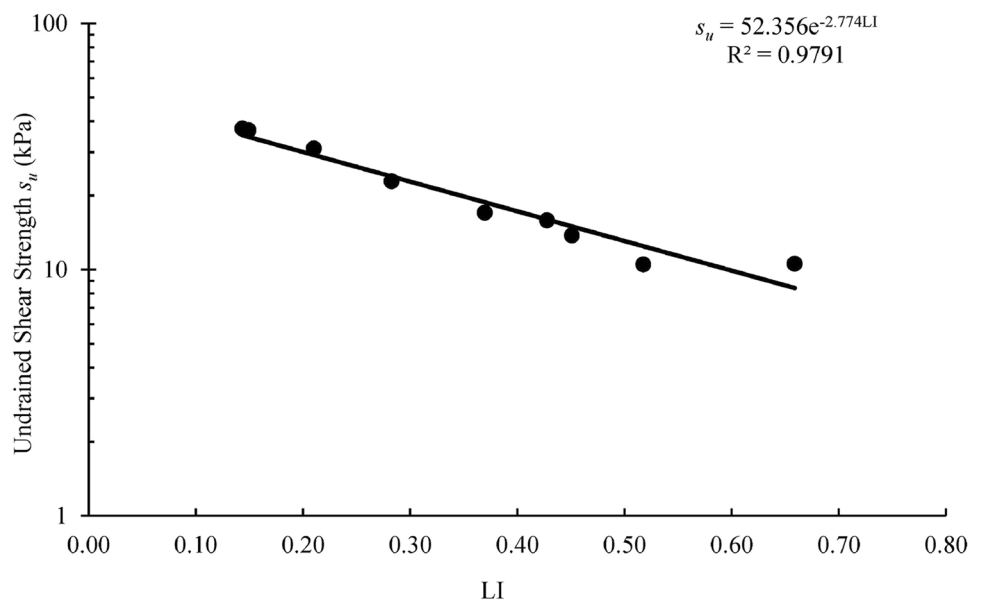
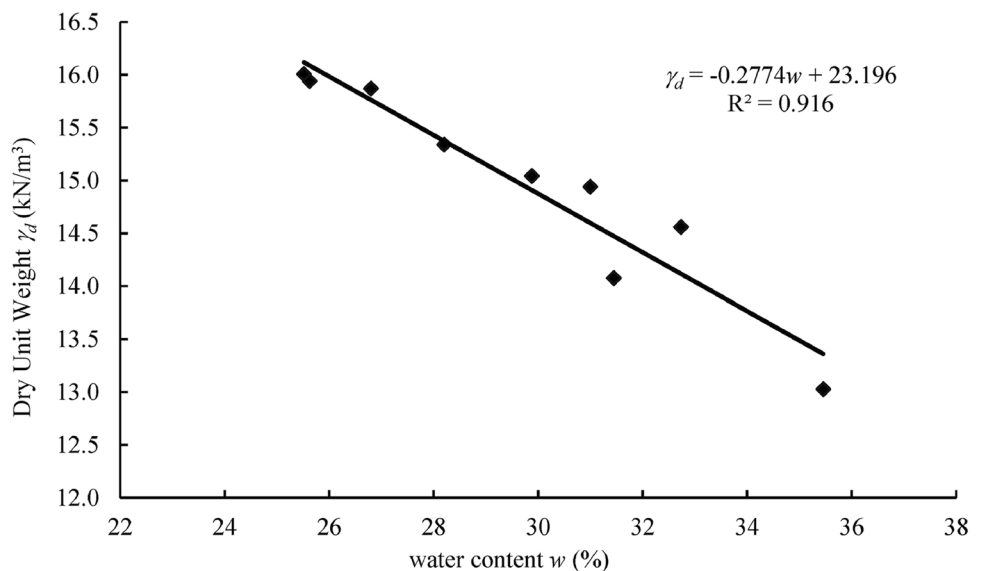


**Fig. 4** Plot of water content (%) and dry unit weight



that  $D_{10}=0.60$  mm,  $D_{30}=3.30$  mm, and  $D_{60}=6.80$  mm as illustrated in Fig. 2. While  $C_u=11.33$ , and  $C_c=2.67$  were calculated. The total percentage of gravels was found to be 58.1%, sand as 39.1%, and fines as 2.8% [38]. The specific gravity was attained as 2.482 from the laboratory tests [39, 40]. The granular material was non-plastic [41] and classified as GW—well graded gravel with sand [42]. MDD was found to be  $19.52$  kN/m<sup>3</sup> at an OMC of 6.8% [31]. The corrected dry unit weight of the material was  $21.51$  kN/m<sup>3</sup> which was at 95% of MDD, and the corrected water content was 3.02% [43]. The direct shear test obtained the  $c=0$  kPa, and  $\phi'=38.4^\circ$ , for particles smaller than 4.75 mm [44]. From the studies, it was predicted that there must be an increase in the effective angle of friction if the small and large-scale direct shear tests are carried out on the same sample. It must be increased to  $5^\circ$  [45], with the range of increase being between  $4^\circ$  and  $5^\circ$  [46]. Therefore,  $\phi'$  was taken as  $43.4^\circ$  in this study. The permeability for the maximum particle size of 4.75 mm was determined to be  $2.020 \times 10^{-4}$  m/s [37], while for  $D_{10}=0.6$  mm the coefficient of permeability was  $1.3 \times 10^{-3}$  m/s [47], which meets the criteria that gravels have the permeability of more than  $1 \times 10^{-3}$  m/s [34]. The summary of the laboratory tests for soft clay and granular material is shown in Table 2.

## Test Setup and Procedure

To carry out the small-scale model tests, the  $500 \times 500 \times 500$  mm mould was constructed from

6-mm-thick mild steel sheets to provide sufficient resistance to lateral deformation during the test. The front of the mould was made transparent by attaching 12.5-mm-thick Plexiglass, which was additionally supported by horizontal bars that were attached to the top and bottom of the mould. The mould was made frictionless by spraying it with paint from the inside. The schematic representation of the experimental setup is shown in Fig. 5. Two types of foundations were used during the test, i.e., strip and square (see Figs. 6 and 7). The 48 mm wide and 148 mm long strip foundation along with 102 mm wide square foundation was used. The foundations were dimensioned so that the mould depth must be more than 6.5 times the width of the strip foundation or 4 times the width of the square foundation so that the stress reaching down to the bottom does not affect the bottom of the mould. The foundations were made of 25 mm thick mild steel (rigid enough) so that they would not bend during the test. To ensure good friction between the foundation and the ground surface, the surface of the foundations was roughened. The scale effect of the grain size was checked from  $B/D_{50}$  and was below 200 for both types of foundations, which has a negligible influence on the bearing capacity [48].

A total of 10 tests were carried out on strip and square foundations by varying the width and depth of the replacement in small-scale modeling. The following tests were performed on strip foundation, (a) only soft clay, (b)  $W=B$ , and  $H=2B$ , (c)  $W=B$ , and  $H=4B$ , (d)  $W=2B$ , and  $H=2B$  and (e)  $W=2B$ , and  $H=4B$ . While the following tests were performed on square foundation, (a) only soft clay, (b)

**Table 2** Summary of laboratory tests

Test	Standard	Soft clay	Granular material
Natural moisture content ( $w$ )	ASTM D 2216	17.67%	–
Specific gravity ( $G_s$ )	ASTM D 854	2.696	2.482
Particle size analysis	ASTM D 6913	Gravel = 1.6%, Sand = 3.9%, and Silt and clay = 94.5%	Gravel = 58.1%, Sand = 39.1%, and Silt and clay = 2.8%
Hydrometer analysis	ASTM D 422	Silt size = 64.5%, and Clay size = 30%	–
Liquid limit (LL)	ASTM D 4318	42.04%	NP
Plastic limit (PL)		22.74%	NP
Plasticity index (PI)		19.30%	NP
Classification of soil (USCS)	ASTM D 2487	CL	GW
95% Maximum dry unit weight ( $\gamma_{dmax}$ )	ASTM D 698	16.06 kN/m <sup>3</sup>	21.51 kN/m <sup>3</sup>
Optimum moisture content (OMC)		15%	3.02%
Undrained shear strength vs. liquidity index ( $s_u$ vs. LI)	ASTM D 2166	For, $s_u = 13$ kPa LI = 0.50 $w = 32\%$	–
Triaxial (UU)	ASTM D 2850	$c = 21.8$ kPa, $\phi = 0^\circ$ , $E = 4671$ kPa	–
Permeability ( $k$ )	ASTM D 5084	$1.009 \times 10^{-9}$ m/s	$1.3 \times 10^{-3}$ m/s [34]
Direct shear test	ASTM D 3080	–	$c = 0$ kPa, $\phi = 43.4^\circ$

**Fig. 5** Schematic representation of small-scale testing program

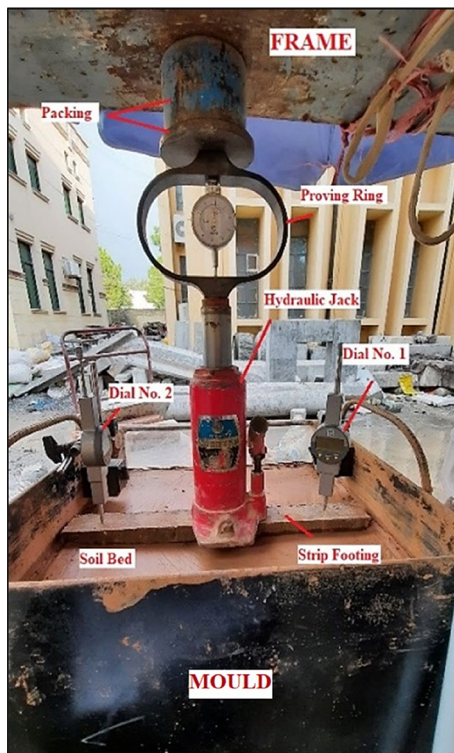
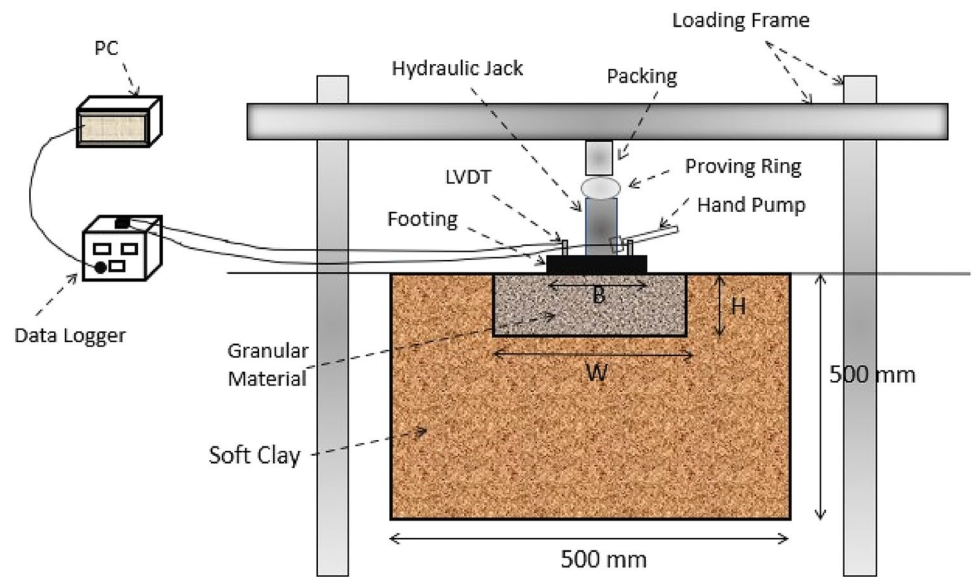


**Fig. 6** Test setup for small-scale model test on strip foundation

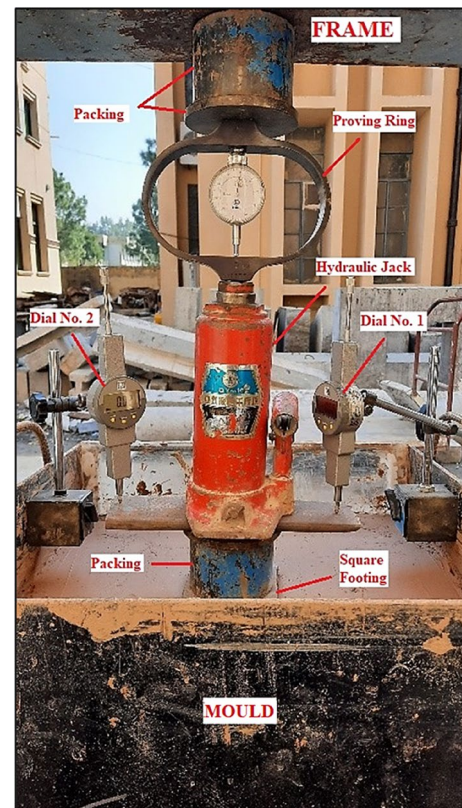


**Fig. 7** Test setup for small-scale model test on square foundation

$W = B$ , and  $H = 1.5B$ , (c)  $W = B$ , and  $H = 3B$ , (d)  $W = 2B$ , and  $H = 1.5B$  and (e)  $W = 2B$ , and  $H = 3B$ . The hydraulic jack with a capacity of 30 kN was used in the test program. Two digital dial gauges with a least count of 0.01 mm and a range of 50 mm with an accuracy of  $\pm 0.04$  mm were used. The right dial was used as dial number 1 and the left side as dial number 2. The load cells with capacities of 5 and 10 kN were

used to measure the applied load. The tests were carried out in 5 min to achieve the undrained conditions by applying a load in equal increments. The tests were terminated when 20% of the foundation width was settled, i.e., 10 mm or 21 mm for strip or square foundations. The dial gauges were placed at opposite ends to average the settlement in case of

irregular settlement on one side. The loading rate varied with each test, for the first test it was 0.6 kN/min. However, since the tests were very sensitive to the loading rate, each test was performed several times to obtain the accurate load–settlement curve at a suitable loading rate relative to that specific test. Therefore, the range of the loading rate for the tests was taken within 0.2–1.4 kN/min.

## Sample Preparation

The soil was prepared at the density of 1459.21 kg/m<sup>3</sup> using 32% water to achieve the undrained shear strength of 13 kPa. In all tests, the mould was filled to 398 mm with the top 102 mm remaining. To prepare the soil bed, a total of 145 kg of the dry mass of soil was required, for this purpose, the soil was divided into five 25 kg and one 20 kg sack. The soil was dried in an oven and then pulverized. The water was added separately to each layer for homogenous mixing. The material was placed in a mould in layers of approximately 69 mm thickness, the last layer was about 40 mm thick. The soft clay was left for curing for 4 days by tightly covering it with a plastic sheet.

After preparing the soft clay bed, the first test was carried out on the strip foundation without any replacement, as shown in Fig. 6. The load was measured with the load cell, while the settlement was measured with two dial gauges. The second test was performed by removing the center of the soil bed until the removal width was 48 mm and the removal depth was 96 mm. The granular material was prepared at the dry unit weight of 21.51 kN/m<sup>3</sup> using 3.02% water. To obtain a homogeneous gradation, the mass was

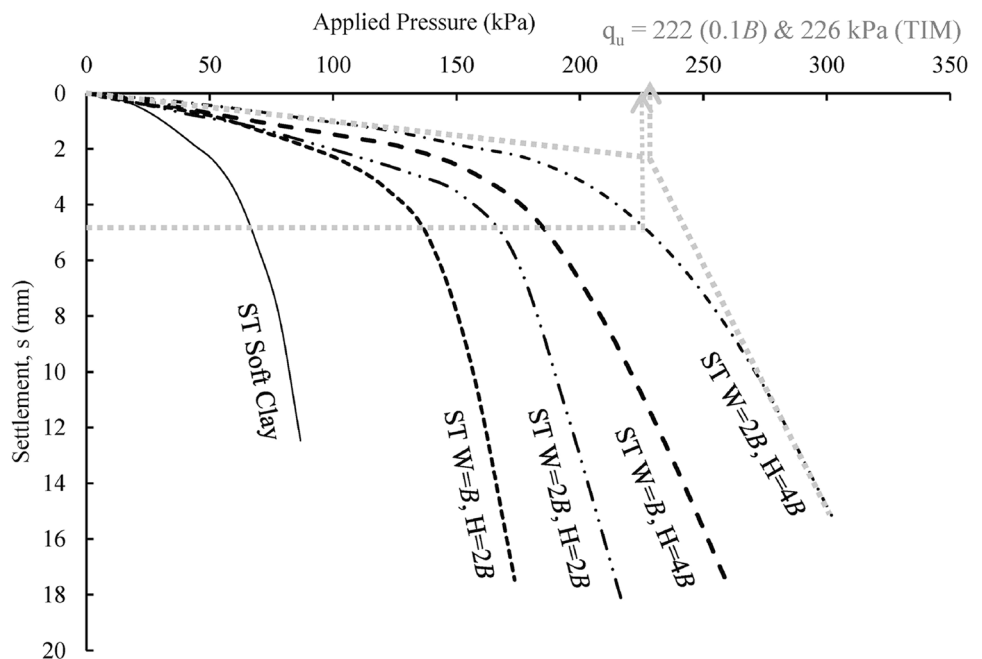
calculated separately for each sieve size. The material was then prepared by mixing appropriately for each sieve size. It was then carefully introduced into the replaced zone and compacted in layers. The experimental setup was then set up for experimentation. All other tests were performed using the same procedure. The experimental setup for the square foundation is shown in Fig. 7.

## Results

The results were obtained from small-scale tests in the form of stress–settlement curves. The curves for strip and square foundations are indicated with a subscript of ‘ST’ and ‘SQ’, respectively. The ultimate bearing capacity with uniaxial loading is usually calculated using two methods. These methods include the tangent intersection method (TIM) [52] and the 0.1*B* method [41]. The deviation of tangents in TIM can lead to deviations of 2–5% in the results [53]. However, it has been observed that the TIM is less accurate than the 0.1*B* method [14]. With the latter method, the load is recorded up to 10% of the foundation width, i.e., 4.8 mm for strip foundations and 10.2 mm for square foundations. As an example, a strip foundation with the width of replacement of 2*B* and the depth of replacement of 4*B* was taken in Fig. 8.

The ultimate bearing capacity according to the 0.1*B* method is obtained by projecting a horizontal line at 4.8 mm and intersecting this with a curve,  $q_u$  was determined to be 222 kPa. For TIM, double tangents were drawn from the beginning and end of the curve and the point of intersection was taken as  $q_u$  which in this case was 226 kPa. Figure 9 represents the stress–settlement curves obtained from

**Fig. 8** Stress vs settlement curves obtained from small-scale model testing for strip (ST) foundation





small-scale tests on a square foundation. As an example,  $W = 2B$  and  $H = 3B$  were taken and the  $q_u$  of 214 kN and 213.57 kN were obtained with TIM and 0.1B methods, respectively. Both methods gave nearly similar results, while the values of  $q_u$  for all remaining tests using both methods are mentioned in Table 4 for comparison.

The comparison of the results of small-scale tests with previous studies leads to the calculation of the dimensionless governing factor  $c_u/\gamma B$ . It was found that  $c_u/\gamma B$  for strip foundations in the present study was almost three times [11] and five times [12] larger than those used previously. It was also observed that the obtained bearing capacity was three and five times higher, suggesting a good agreement of the results. Studies [13, 16] used a higher value of  $c_u/\gamma B$ , showing that the strong material was used in the test program, while the obtained results showed smaller  $q_u$  values as compared to this study.

## Numerical Modeling

In this study, a total of 87 numerical modeling tests were carried out on foundations with PLAXIS 2D V8. It is a finite element software for analyzing the model for deformation and stability [49]. 41 tests were performed on strip foundation by taking four widths of replacement as  $B$ ,  $1.5B$ ,  $2B$ , and  $2.5B$ . For each width of replacement, the depth ratio of  $H/B = 0.5, 1, 1.5, 2, 2.5, 3, 3.5, 4, 4.5,$  and  $5$  was changed. Similarly, 46 tests were performed on a square foundation with five widths of replacements as  $B$ ,  $1.5B$ ,  $2B$ ,  $2.5B$ , and  $3B$  and variations in depth ratios from  $0.5B$  to  $4.5B$ . In this study, the plane strain modeling technique with 15 nodal

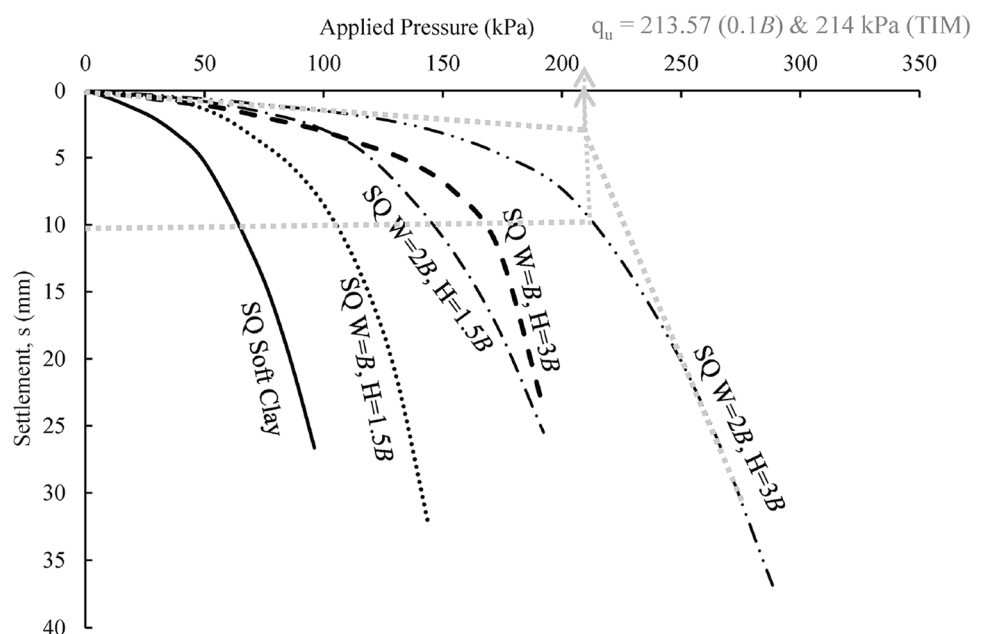
triangular elements and Mohr-Coulombs failure criteria was used [50]. It has been suggested by some researchers that the behaviour of the clay can be adequately modeled with the appropriate cohesion value and the MC model [51].

The tests were carried out on the assumption that the water table had no effect on the model. This resulted in the same unsaturated and saturated unit weight for both geomaterials. The bulk unit weight  $\gamma_b$  was used as  $\gamma_{\text{unsat}}$  and  $\gamma_{\text{sat}}$ . The bulk unit weight for soft clay and granular material from the laboratory tests was obtained as  $18.89 \text{ kN/m}^3$  and  $22.16 \text{ kN/m}^3$ , respectively. The elastic modulus for soft clay was calculated from the stress–strain graphs obtained from triaxial and unconfined compression tests was 4700 kPa. Whereas for granular material,  $E$  was assumed to be 47,000 kPa when taken in a loose state [52, 53] to have the rigid layer.

PLAXIS automatically assumed a poisson value of 0.495 for the undrained behavior of soft clay. While  $\nu$  of 0.3 was used for gravels. The dilatancy angle  $\psi$  was taken as zero for soft clay, while it was calculated using expression  $\psi = \phi' - 30^\circ$  [54] for granular material, and the value of  $13.4^\circ$  was obtained. The reduction factor  $R$  for the interaction of rough steel and granular material was determined to be 0.8, and for the interaction of rough steel and clay was 0.5 [55]. Table 3 shows the summary of the parameters used for the numerical analysis.

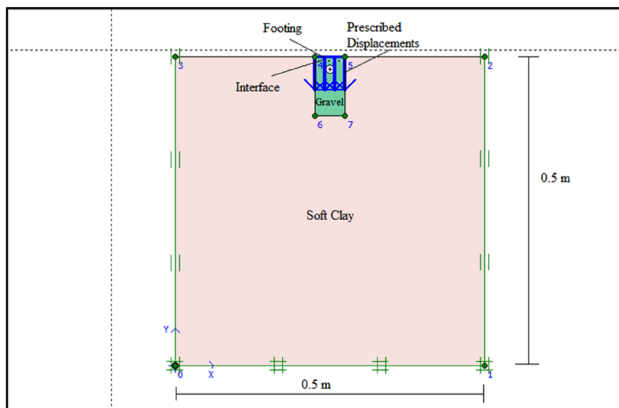
The steel foundations were used as plate material with elastic properties in the FEM modeling. The material properties of the plate included the flexural rigidity (bending stiffness)  $EI$  and the axial stiffness  $EA$ . The modulus of elasticity  $E$  of steel was assumed to be 206.7 GPa and the poisson ratio  $\nu$  was taken as 0.3 [56].  $EA$  was obtained as  $5.168 \times 10^6 \text{ kN/m}$  and  $EI$  as  $2.691 \times 10^2 \text{ kNm}^2/\text{m}$ . The

**Fig. 9** Stress vs settlement curves obtained from small-scale model testing for square (SQ) foundation



**Table 3** Summary of parameters used in numerical analysis

Material	$\gamma_{\text{unsat}}/\gamma_{\text{sat}}$ (kN/m <sup>3</sup> )	$E$ (kPa)	$c$ (kPa)	$\nu$	$\varphi$	$\psi$	$k_x, k_y$ (m/day)	$R_{\text{interface}}$
Soft clay	18.8	4700	13	0.35	0°	0°	$8.718 \times 10^{-5}$	0.5
Granular material	22.16	47,000	0.18	0.3	43.4°	13.4	112.36	0.8

**Fig. 10** Geometry of model (strip foundation,  $W=B$ ,  $H=2B$ )

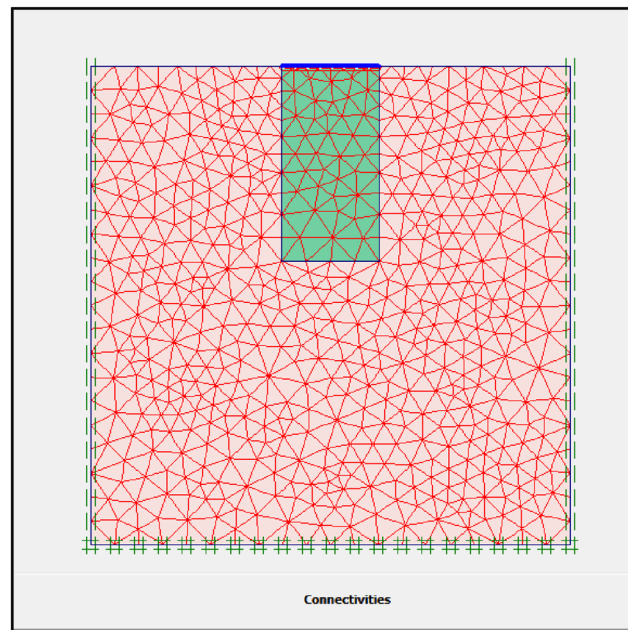
specific weight per unit length of steel was 1.9625 kN/m<sup>2</sup> calculated from its weight density of 78.5 kN/m<sup>3</sup>.

## Numerical Procedure

For the FEM modeling in PLAXIS, the coordinates of the geometry were calculated and drawn together with the foundation. The materials and foundation properties were assigned to the respective areas. The prescribed displacements were distributed over the foundation area. The settlements were carried up to 20% of the foundation width, this was considered to be the point at which the significant influence of the load can be observed. For the strip and square foundations, the vertical prescribed displacements of 10 mm and 21 mm were assigned with zero horizontal prescribed displacement. The model was fixed from all three sides by fixing the boundaries, as shown in Fig. 10. A very fine mesh was used to analyze the models, as shown in Fig. 11. Additional parameters were increased to a maximum of 10,000 steps To obtain accurate results [51].

## Numerical Results

The extent of the vertical displacements was investigated using four cases with a square foundation (i) only soft clay, (ii)  $W=B$ ,  $H=1.5B$ , (iii)  $W=B$ ,  $H=3B$ , and (iv)  $W=2B$ ,  $H=1.5B$  as shown in Fig. 12. The vertical displacements in case 1 were at a maximum just below the foundation shown in red in Fig. 12a. They were negligible in the center and bottom of the mould, as the load influence did not reach the bottom of the mould. In this case, a local shear failure was

**Fig. 11** Undeformed mesh after analysis (strip foundation  $W=B$ ,  $H=2B$ )

observed [57]. For case 2, the width of replacement was taken as  $B$  and the depth of replacement as  $1.5B$ , a punching failure through replaced zone was observed [1]. In addition, the loading effect did not reach the bottom as there were negligible vertical displacements at the bottom, as in Fig. 12b.

In case 3, the effect of the depth of replacement was examined by taking  $H$  as  $3B$ , and it was found that the vertical displacements were observed at a greater depth as shown in Fig. 12c. It can also be seen that a narrower but deeper area with displacements was found in the area of the replacement zone, which in this case emphasizes the punching shear failure through replaced zone [1]. In case 4, the effect of the replaced width was examined assuming  $W=2B$ , and it was observed that a wider area under the foundation was affected by the load. The failure of the distributed foundation was observed in this case as shown in Fig. 12d [2]. The maximum displacements were mainly observed in the replaced zone but the area of failure zone was less than the area of the replaced zone. It was concluded that by increasing the depth of replacement, the improvement in the load-bearing capacity is more significant than increasing the width of replacement.

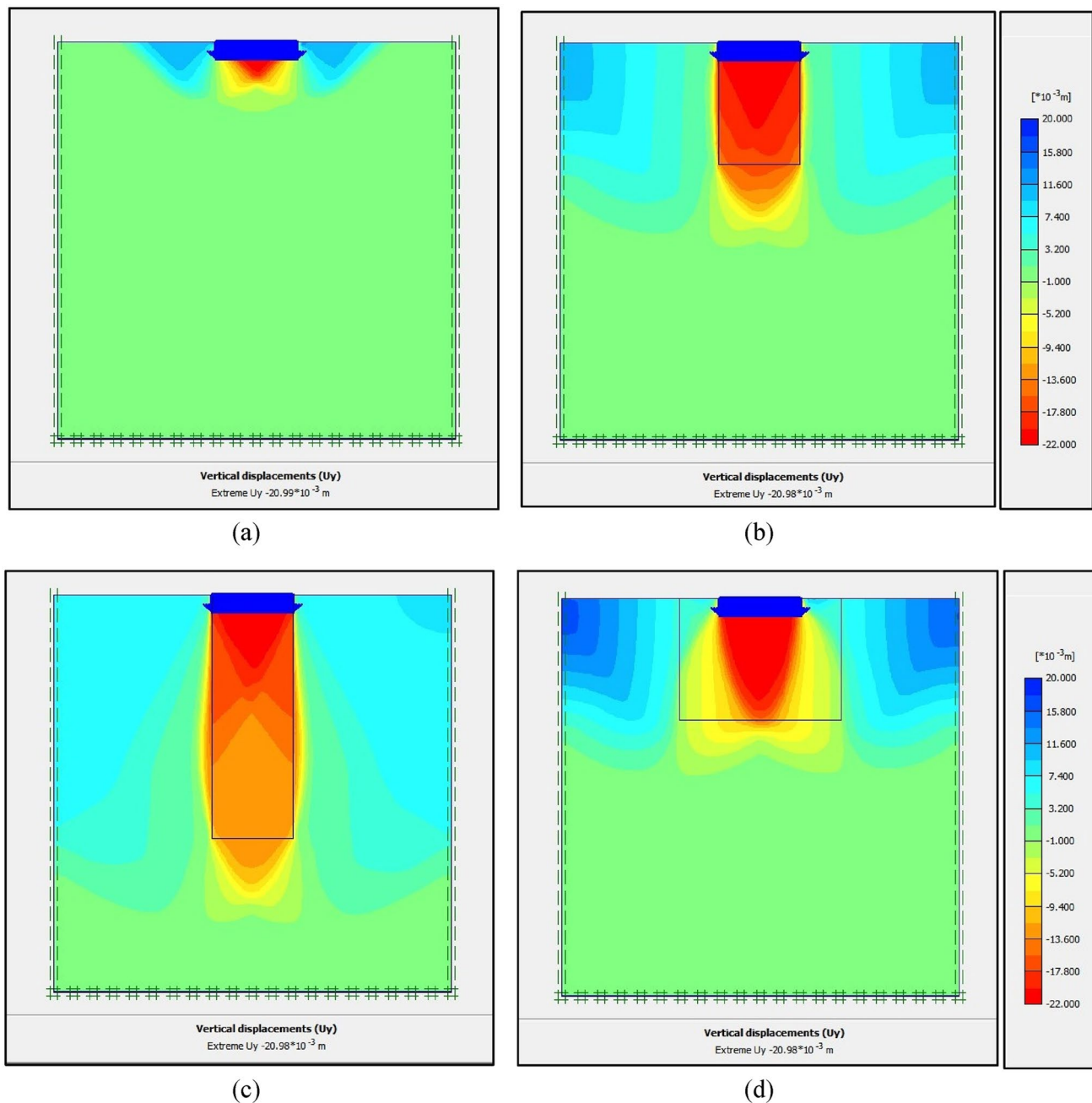


**Fig. 12** Vertical displacements. **a** Case i: square foundation on soft clay, **b** Case ii: square foundation with  $W=B$ ,  $H=1.5B$ , **c** Case iii: square foundation with  $W=B$ ,  $H=3B$ , **d** case iv: square foundation with  $W=2B$ ,  $H=1.5B$

The stress–settlement graphs were obtained from 41 model tests of strip foundations, carried out with FEM modeling in PLAXIS 2D V8. The model tests were carried out by varying four widths of replacements and ten depth ratios. The results of strip foundations with the width of replacement  $W=B$  and  $W=2B$  at different depth ratios are shown in Figs. 13 and 14. The demonstration of the tangent intersection method (TIM) was carried out for  $W=B$  and  $H/B=1.5$ . It can be seen that the load-bearing capacity calculated using

this method is 124 kPa, while from the  $0.1B$  method it was 120.88 kPa, measured at 4.8 mm, as shown in Fig. 13.

The stress–settlement graphs for square foundations with the width of replacement of  $B$  and  $2B$  at different depth ratios are shown in Figs. 15 and 16. These graphs were produced by running 46 model tests on software with five and nine different widths and depths of replacements, respectively. For the depth ratio of 1, Fig. 15 shows that TIM achieved the ultimate bearing capacity of 100 kPa. While the

**Fig. 13** Stress settlement curves of strip foundation with  $W=B$  at different depth ratios

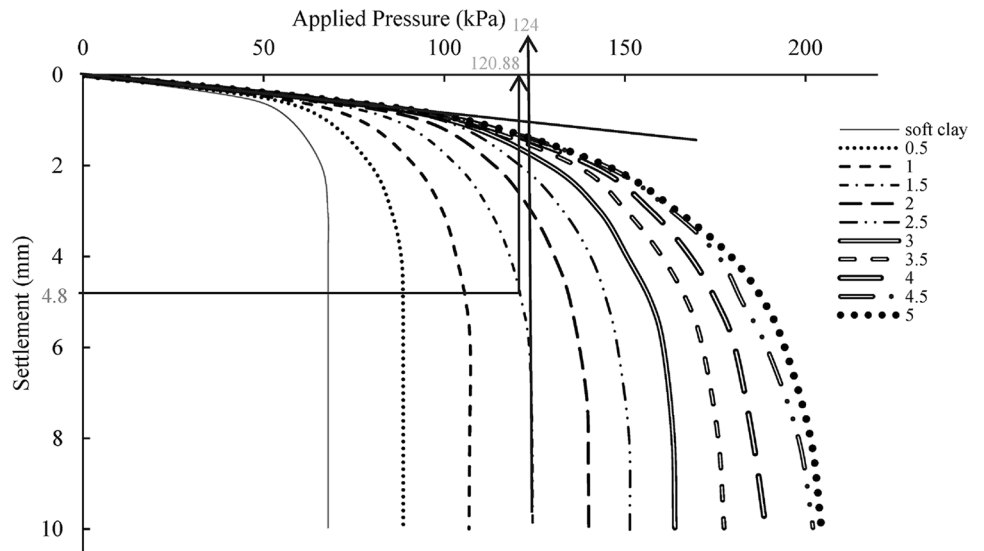


**Fig. 14** Stress settlement curves of strip foundation with  $W=2B$  at different depth ratios

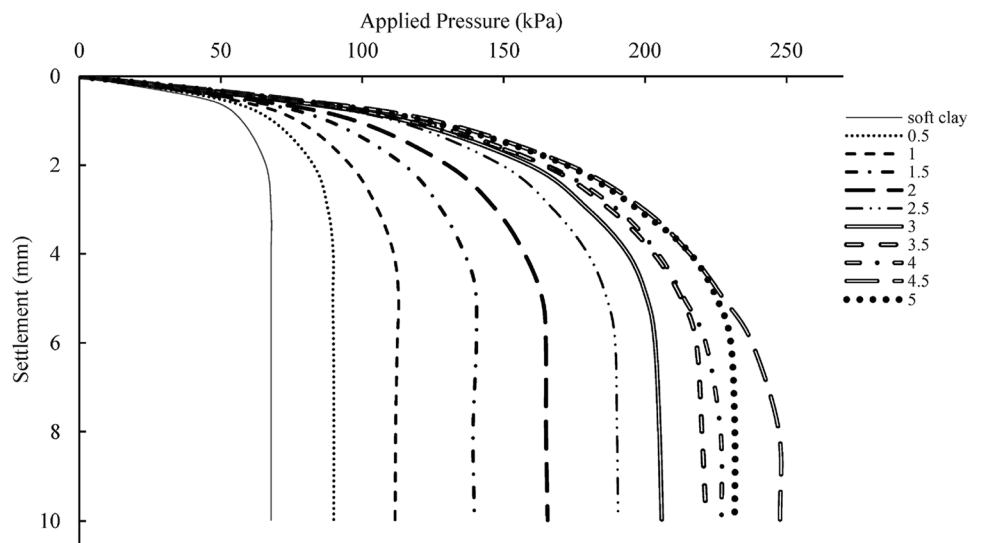


**Fig. 15** Stress settlement curves of square foundation with  $W=B$  at different depth ratios

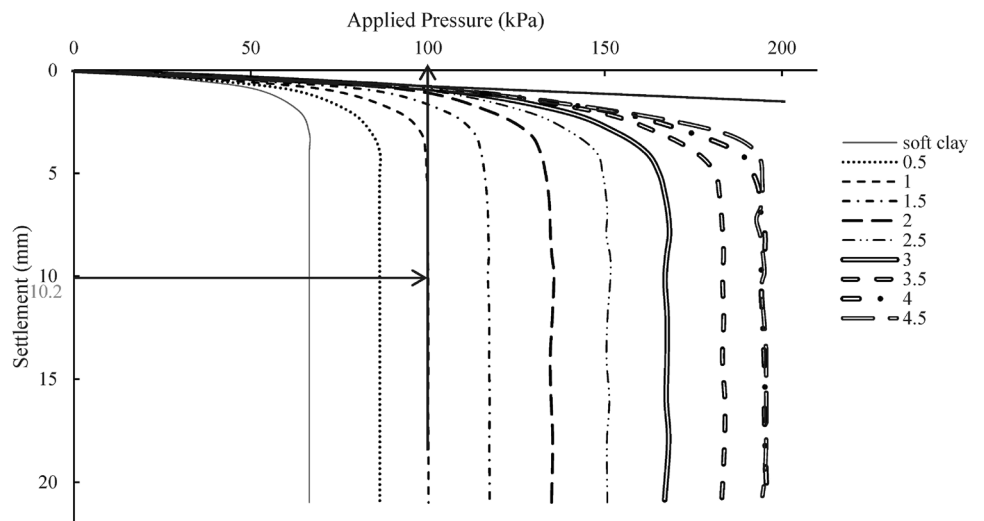
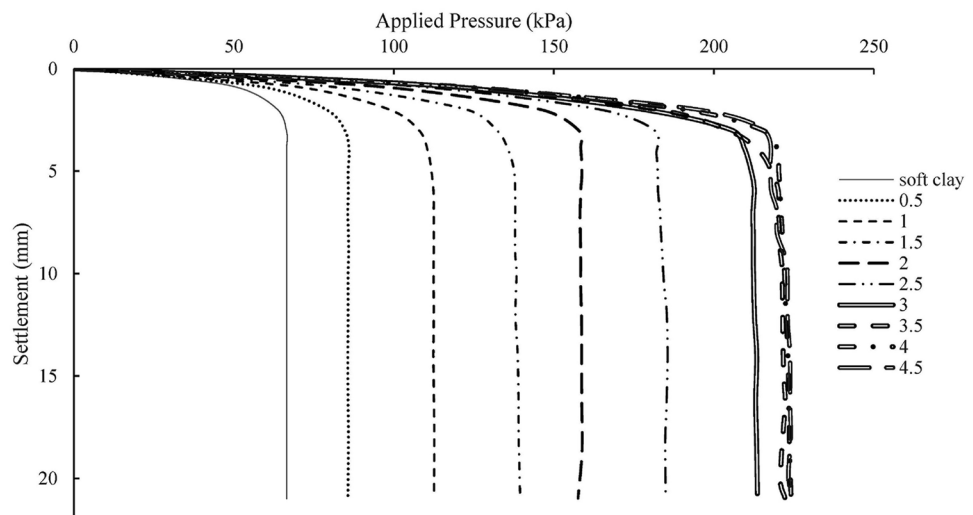




**Fig. 16** Stress settlement curves of square foundation with  $W=2B$  at different depth ratios



0.1B method obtained 100.12 kPa against the settlement of 10.2 mm for a square foundation.

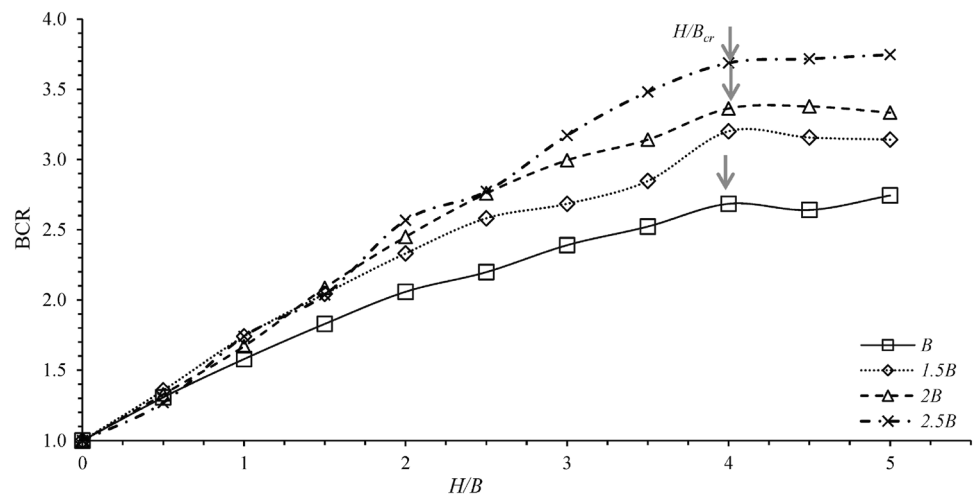
The results obtained from the numerical analysis indicated that the bearing capacity is significantly increased due to an increase in the width and depth of replacement. A dimensionless factor known as bearing capacity ratio (BCR) was used to describe the extent of improvement of bearing capacity. BCR is the ratio of the bearing capacity after replacement to the bearing capacity of the soil without replacement [58].

In the case of a strip foundation, using the tangent intersection and 0.1B methods, there was an increase in BCR for every 0.5B increase in the width of replacement. The increase in BCR was significant after the 1.5 depth ratio. The point at which the improvement in BCR was insignificant was taken as the critical depth ratio  $H/B_{cr}$  [59] that was apparent for each width of replacement. The critical depth ratio was found to be 4 for all widths of replacements,

i.e.,  $B$ ,  $1.5B$ ,  $2B$ , and  $2.5B$ , as shown in Figs. 17 and 18. No recommended width of replacement was found, as the BCR increases steadily with every increase in width of replacement.

In the case of square foundation, the BCR increased significantly with increasing the width of replacement. The increase in  $H/B$  was steep after  $H/B$  of 2. For the first curve, i.e., when the width of replacement  $W$  was equal to the width of the foundation  $B$ , the increase in the bearing capacity ratio was noted till  $H/B_{cr}$  of 4. In the second phase, when the width of the replacement was increased to 1.5 times the width of the foundation,  $H/B_{cr}$  was measured to be 3.5. In all three remaining phases of the numerical model tests, the  $H/B_{cr}$  was found to be 3, as shown in Fig. 19. For the critical width of replacement, the graph shows that a significant increase in BCR was observed up to  $2B$ , after which the increase in BCR was insignificant. It can be seen from Fig. 19, that the recommended depth

**Fig. 17**  $H/B$  vs. BCR of strip foundation (tangent intersection method—TIM)



ratio is 3, and the width of replacement is  $2B$ . Figure 20 shows the  $H/B$  vs. BCR for different widths of

replacement using the  $0.1B$  method. It showed the same trend as TIM with minor differences in the BCR values.

**Fig. 18**  $H/B$  vs. BCR of strip foundation ( $0.1B$  method)

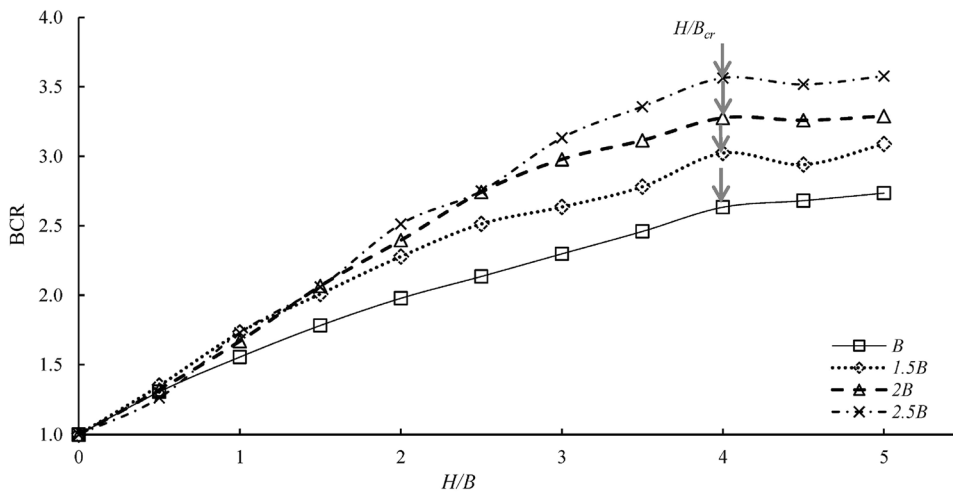


**Fig. 19**  $H/B$  vs. BCR of square foundation (tangent intersection method—TIM)

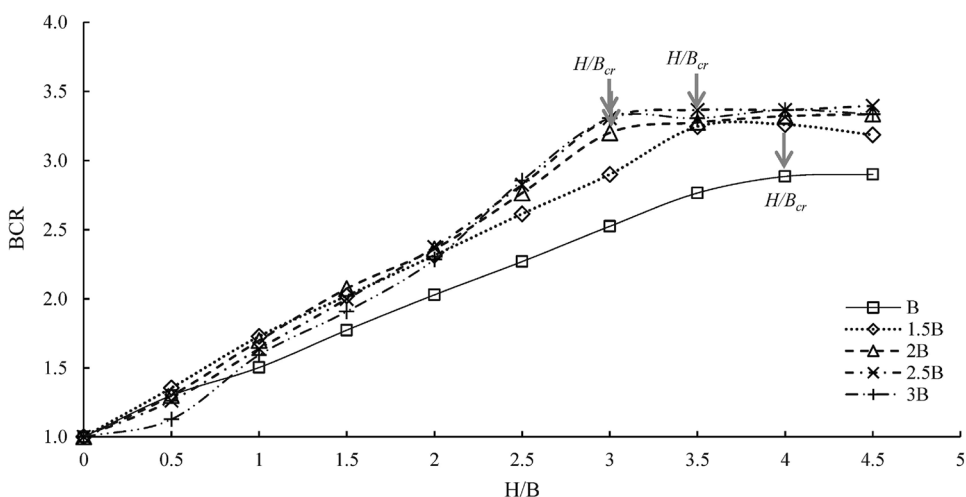


**Fig. 20**  $H/B$  vs. BCR of square foundation ( $0.1B$  method)

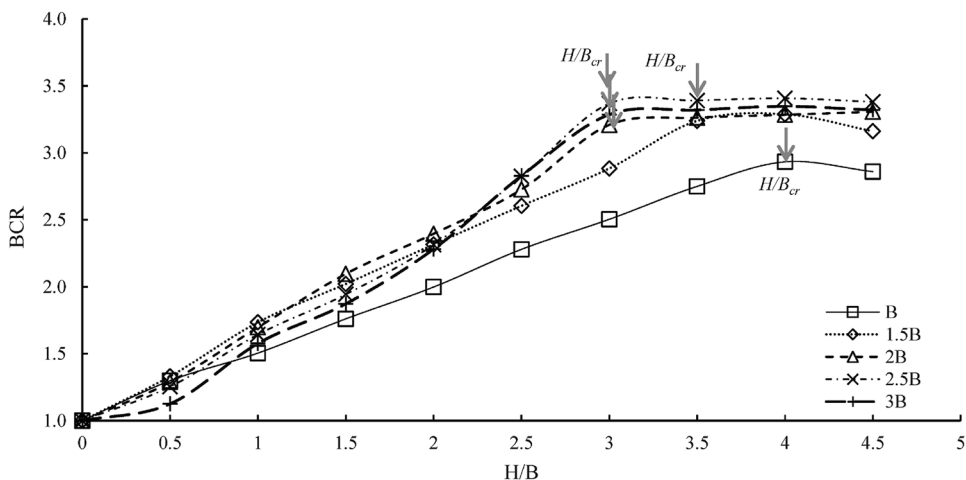


**Table 4** Validation of  $q_u$  from experimental and software analyses

Type of foundation	Test no.	Description	Experimental model tests		PLAXIS 2D analysis		% Age difference	
			TIM (kPa)	0.1B method (kPa)	TIM (kPa)	0.1B method (kPa)	TIM (%)	0.1B method (%)
Strip foundation	1	Soft clay only	67	67	67.8	67.8	1.18	1.18
	2	Replacing $W=B$ , and $H=2B$	143	137	139.5	134.16	2.51	2.12
	3	Replacing $W=B$ , and $H=4B$	183	183	182	178.6	0.55	2.46
	4	Replacing $W=2B$ , and $H=2B$	166	167	166	162.48	0.00	2.78
	5	Replacing $W=2B$ , and $H=4B$	226	222	228	222.2	0.88	0.09
Square foundation	6	Soft clay only	67	70	66.55	66.55	0.68	5.18
	7	Replacing $W=B$ , and $H=1.5B$	118	115	118	117.15	0.00	1.84
	8	Replacing $W=B$ , and $H=3B$	165	167	168	166.63	1.79	0.22
	9	Replacing $W=2B$ , and $H=1.5B$	138	145	138	139.5	0.00	3.94
	10	Replacing $W=2B$ , and $H=3B$	214	213	213	213.57	0.47	0.27

### Comparison of FEM and Experimental Testing

For strip foundations on clayey soil replaced with sand (SP) and geosynthetic reinforcement [12], loose sand replaced with dense sand [21], and dense sand with geosynthetic reinforcement [25], showed the similarity in the experimental and PLAXIS results. While for circular foundations on problematic clay and well-graded, gravel–silty gravel (GW–GM), the validation of the large-scale results with small-scale and FEM analyzes showed a good comparison [26]. It was also observed that the scale effect has no significant effect on the analysis, and can therefore be neglected [51]. The other two types of replacement materials, medium to loose and very dense sand in clay also showed a good comparison of the results between both types of analysis [60].

The results of the experimental tests and PLAXIS modeling were compared in Table 4, for strip and square foundations. The results were equated by calculating the percentage difference in ultimate bearing capacities from the TIM and 0.1B method. TIM showed a deviation of up to 2.51% in the results, while 0.22–5.18% of the variation from the 0.1B method was obtained between both small-scale and FEM modeling techniques. The percentage differences obtained by both methods are in good agreement with the results of previous studies as discussed above.

### Conclusion

The study was carried out for strip and square foundations, which were underlaid with soft clay on granular material. The extent of the replacement was examined and the following conclusions were drawn.

- The results of the small-scale tests were compared and validated using FEM software and there was good agreement between the results.
- The bearing capacity was calculated using two methods i.e., Tangent Intersection and 0.1B method, and both methods gave almost similar results.
- The BCR increases significantly with the increasing width of the replacement, for both types of foundations, which can be observed after the depth ratio  $H/B$  of 1.5 for strip foundation and 2.5 for the square foundation.
- The depth of replacement of  $3B$  and width of replacement of  $2B$  was recommended for a square foundation.
- For strip foundation, the recommended depth of replacement was found at  $4B$ . However, no significant point was obtained for the width of the replacement. Because of each increment of increase in the width of the replacement, there was a steady increase in the BCR.
- After the depth of replacement of  $3B$  and  $4B$  for square and strip foundations, the soil behaved as if it were only placed on the replaced layer.
- It turned out that the depth of replacement is a more important factor in improving the load-bearing capacity than the width of the replacement.

**Author Contributions** The main idea was conceptualized by ZBM and SMJ, while the methodology was defined by ZBM and BA. The material was collected by ZBM. The experimental part was implemented by ZBM with the help of DU under the supervision of BA. The original draft was prepared by ZBM with help of DU. The review of the manuscript was done by BA. The overall work was carried out under the supervision of BA and SMJ.

**Funding** This research received no external funding.

**Data Availability** All data, models, and code generated or used during the study appear in the submitted article.

## Declarations

**Conflict of interest** The authors declare that there is no conflict of interest regarding the publication of this article.

**Originality statement** The manuscript of this paper, even with a minor overlap with text, research objectives, presentation of research data, figures/photographs, tables, research findings, conclusions, etc., has not been submitted to any other journal for simultaneous consideration. Also, no part of this paper manuscript has been published earlier by me/us and others at any publication platform (technical journal, conference proceedings, magazine, newspaper, etc.). The details as reported in this paper are truly my/our unpublished original research work in all aspects.

## References

- Lawton EC (2001) Section 6A “Soil Improvement and Stabilization”, Practical Foundation Engineering Handbook. McGraw-Hill, New York
- Han J (2015) Principles and practice of ground improvement. Wiley, New York
- Madhav MR, Vitkar PP (1978) Strip footing on weak clay stabilized with a granular trench or pile. *Can Geotech J* 15:600–605. <https://doi.org/10.1139/t78-066>
- Abhishek SV, Rajyalakshmi K, Madhav MR (2014) Bearing capacity of strip footing on reinforced foundation bed over soft ground with granular trench. *Indian Geotech J* 45:304–317. <https://doi.org/10.1007/s40098-014-0138-y>
- Michalowski RL, Shi L (1995) Bearing capacity of footings over two-layer foundation soils. *J Geotech Eng* 121:421–428. [https://doi.org/10.1061/\(ASCE\)0733-9410\(1995\)121:5\(421\)](https://doi.org/10.1061/(ASCE)0733-9410(1995)121:5(421))
- Bai X-H, Huang X-Z, Zhang W (2013) Bearing capacity of square footing supported by a geobelt-reinforced crushed stone cushion on soft soil. *Geotext Geomembr* 38:37–42. <https://doi.org/10.1016/j.geotextmem.2013.04.004>
- Hemalatha A, Mahendran N, Ganesh Prabhu G (2014) Prediction of effects of geogrid reinforced granular fill on the behaviour of static liquefaction. *Adv Mater Sci Eng* 2014:1–11. <https://doi.org/10.1155/2014/210843>
- Ornek M, Laman M, Demir A, Yildiz A (2012) Prediction of bearing capacity of circular footings on soft clay stabilized with granular soil. *Soils Found* 52:69–80. <https://doi.org/10.1016/j.sandf.2012.01.002>
- Zhang W, Du D, Bai X (2018) In situ testing of square footing resting on geobelt-reinforced gravel thin cushion on soft silt. *Adv Mater Sci Eng* 2018:1–12. <https://doi.org/10.1155/2018/3563914>
- Hamed H (1986) Bearing capacity of strip foundation on a granular trench in soft clay, University of Texas. El Paso. <https://doi.org/10.4203/ccp.9.18.5>
- Khing KH, Das BM, Puri VK, Yen SC, Cook EE (1993) Foundation on strong sand underlain by weak clay with geogrid at the interface. *Geotext Geomembr* 13:199–206. [https://doi.org/10.1016/0148-9062\(95\)90238-4](https://doi.org/10.1016/0148-9062(95)90238-4)
- Lee KM, Manjunath VR, Dewaiker DM (1999) Numerical and model studies of strip footing supported by a reinforced granular fill–soft soil system. *Can Geotech J* 36:793–806. <https://doi.org/10.5860/choice.41-2927.14>
- Rethaliya RP, Verma AK (2009) Strip footing on sand overlying soft clay with geotextile interface. *Indian Geotech J* 39:271–287
- Kolay PK, Kumar S, Tiwari D (2013) Improvement of bearing capacity of shallow foundation on geogrid reinforced silty clay and sand. *J Constr Eng* 2013:1–10. <https://doi.org/10.1155/2013/293809>
- Fattah MY, Al-Waily MJM (2015) Bearing capacity of foundations resting on a trench of local reclaimed asphalt pavement material. *Glob J Eng Sci Res Manag* 2:90–105
- Dalaly NK, Al-Soud MS, Abdul Jabar SS (2015) A new technique of strengthening soft soil under a strip footing by a granular trench reinforced with geogrid micro mesh. *Aust J Civ Eng* 13:11–21. <https://doi.org/10.1080/14488353.2015.1092633>
- Fattah MY, Al-Neami MA, Al-Suhaily AS (2015) Improvement of bearing capacity of footings on soft clay by partial soil replacement technique. 2nd International conference on building, construction, environmental engineering
- Likitlersuang S, Surarak C, Wanatowski D, Oh E, Suwansawat S, Balasubramaniam A (2014) Simplified finite-element modelling for tunnelling-induced settlements. *Geotech Res* 1:133–152. <https://doi.org/10.1680/gr.14.00016>
- Likitlersuang S, Surarak C, Wanatowski D, Oh E, Balasubramaniam A (2013) Finite element analysis of a deep excavation: a case study from the Bangkok MRT. *Soils Found* 53:756–773. <https://doi.org/10.1016/j.sandf.2013.08.013>
- Likitlersuang S, Chheng C, Surarak C, Balasubramaniam A (2018) Strength and stiffness parameters of Bangkok clays for finite element analysis. Author Downloaded from Griffith Research Online Strength and Stiffness Parameters of Bangkok Clays for Finite Element Analysis. <https://doi.org/10.1016/j.sandf.2012.07.009>
- Unnikrishnan N, Johnson AS, Rajan S (2010) Response of strip footings supported on granular trench. In: Indian geotechnical conference, pp 525–528
- Unnikrishnan N, Rajan S, Johnson AS (2011) Bearing capacity of strip footings on encapsulated granular trenches. In: Indian geotechnical conference
- Kumar J, Chakraborty M (2015) Bearing capacity of a circular foundation on layered sand-clay media. *Soils Found* 55:1058–1068. <https://doi.org/10.1016/j.sandf.2015.09.008>
- Gupta R, Trivedi A (2009) Bearing capacity and settlement of footing resting on confined loose silty sands. *Electron J Geotech Eng* 14A:1–17
- Aparna SR, Unnikrishnan N (2016) Behaviour of strip footing supported on stressed encapsulated granular trenches. *Int J Innov Res Sci Eng Technol* 5:292–302
- Hasanzadeh A, Choobbasti AJ (2016) Estimation of bearing capacity of circular footings on clay stabilized with granular soil: case study. *Int J Civ Eng Geo-Environ* 6:47–54
- Fattah MY, Al-Baghdadi W, Omar M, Shanableh A (2010) Analysis of strip footings resting on reinforced granular trench by the finite element method. *Int J Geotech Eng* 4:471–482. <https://doi.org/10.3328/ijge.2010.04.04.471-482>
- Bouassida M, Jellali B, Lyamin A (2014) Ultimate bearing capacity of a strip footing on ground reinforced by a trench. *Int J Geomech* 15:1–8. [https://doi.org/10.1061/\(ASCE\)GM.1943-5622.0000418](https://doi.org/10.1061/(ASCE)GM.1943-5622.0000418)
- Ranjbar A, Golshani AA (2018) The effect of granular trench’s depth on bearing capacity of shallow foundations on the soft ground. *J New Approach Civ Eng* 2:39–48. <https://doi.org/10.30469/JNACE.2018.69393>



30. Bhattacharya P, Kumar J (2017) Bearing capacity of foundations on soft clays with granular column and trench. *Soils Found* 57:488–495. <https://doi.org/10.1016/j.sandf.2017.05.013>
31. ASTM D 698 (2009) Standard test methods for laboratory compaction characteristics of soil using standard effort (12400 ft-lbf/ft<sup>3</sup> (600 kN-m/m<sup>3</sup>)), 1–13. <https://doi.org/10.1520/D0698-12R21>
32. ASTM D 2216 (2000) Standard test method for unconfined compressive strength of cohesive soil, 1–6. <https://doi.org/10.1520/D2166-00>
33. Wroth CP, Wood DM (1978) The correlation of index properties with some basic engineering properties of soils. *Can Geotech J* 15:137–145
34. Terzaghi K, Peck RB, Mesri G (1996) *Soil mechanics in engineering practice*, 3rd edn. Wiley, New York
35. Cerato AB, Lutenegeger AJ (2005) Bearing capacity of square and circular footings on a finite layer of granular soil underlain by a rigid base. *J Geotech Geoenviron Eng* 132:1496–1501. [https://doi.org/10.1061/\(ASCE\)1090-0241\(2006\)132:11\(1496\)](https://doi.org/10.1061/(ASCE)1090-0241(2006)132:11(1496))
36. ASTM D 2850 (2003) Standard test method for unconsolidated-undrained triaxial compression test on cohesive soils, 1–6. <https://doi.org/10.1520/D2850-15>
37. ASTM D 5084 (2010) Standard test methods for measurement of hydraulic conductivity of saturated porous materials using a flexible wall permeameter, 1–24. <https://doi.org/10.1520/D5084-10>
38. ASTM D 6913 (2004) Standard test methods for particle-size distribution (gradation) of soils using sieve, 1–34. <https://doi.org/10.1520/D6913-04R09E01.2>
39. ASTM C 127 (2007) Standard test method for density, relative density (specific gravity), and absorption of coarse aggregate, 1–7. <https://doi.org/10.1520/C0127-15>
40. ASTM D 854 (2002) Standard test methods for specific gravity of soil solids by water pycnometer, 1–7. <https://doi.org/10.1520/D0854-14>
41. ASTM D 4318 (2000) Standard test methods for liquid limit, plastic limit, and plasticity index of soils, 1–14. <https://doi.org/10.1520/D4318-17E01>
42. ASTM D 2487 (2000) Standard practice for classification of soils for engineering purposes (unified soil classification system), 04:1–12. <https://doi.org/10.1520/D2487-17E01>
43. ASTM D 4718 (1987) Standard practice for correction of unit weight and water content for soils containing oversize particles, 1–3. <https://doi.org/10.1520/D4718-87R07.2>
44. ASTM D 3080 (2011) Standard test method for direct shear test of soils under consolidated drained, 1–9. <https://doi.org/10.1520/D3080>
45. Alias R, Kasa A, Taha MR (2014) Particle size effect on shear strength of granular materials in direct shear test. *Int J Civ Archit Struct Constr Eng* 8:1084–1087. <https://doi.org/10.5281/zenodo.1096805>
46. Nakao T, Fityus S (2008) Direct shear testing of a marginal material using a large shear box. *Geotech Test J* 31:10. <https://doi.org/10.1520/GTJ101237>
47. NAVFAC (1986) *Soil Mechanics Design Manual 7.01*, 7.1-139
48. Habib PA (1974) Scale effect for shallow footings on dense sand. *J Geotech Geoenviron Eng* 100:95–99
49. Brinkgreve RBJ, Broere W, Waterman D (2004) *Plaxis finite element code for soil and rock analysis, 2D—Version 8*
50. Cicek E, Guler E (2015) Bearing capacity of strip footing on reinforced layered granular soils. *J Civ Eng Manag* 21:605–614. <https://doi.org/10.3846/13923730.2014.890651>
51. Ornek M, Demir A, Laman M, Yildiz A (2012) Numerical analysis of circular footings on natural clay stabilized with a granular fill. *ACTA Geotech Slov* 1:61–75
52. Obrzud RIF, Truty A (2018) *The hardening soil model—a practical guidebook Z soil*, 71
53. AASHTO (2012) *AASHTO LRFD Bridge Design Specifications*, American Association of State Highway and Transportation Officials, Washington, DC
54. Bolton MD (1986) The strength and dilatancy of sands. *Geotechnique* 36:65–78. <https://doi.org/10.1680/geot.1986.36.1.65>
55. Potyondy JG (1961) Skin friction between various soils and construction materials. *Géotechnique* 11:339–353. <https://doi.org/10.1680/geot.1961.11.4.339>
56. Chen S-L, Li S-F, Fang S-F (1994) Elastoplastic large deflection analysis of cold-formed members using spline finite strip method. In: *Twelfth international special conference on cold-formed steel structures*, St. Louis, pp 251–263
57. Vesic AS (1973) Analysis of ultimate loads of shallow foundations. *J Soil Mech Found Div* 99:45–73
58. Binquet J, Lee KL (1975) Bearing capacity tests on reinforced earth slabs. *J Geotech Eng Div* 101:1241–1255
59. Al-Shenawy AO, Al-karni A (2005) Derivation of bearing capacity equation for a two layered system of weak clay layer overlaid by dense sand layer. *Pertanika J Sci Technol* 13:213–235
60. Ismail Ibrahim KMH (2014) Bearing capacity of circular footing resting on granular soil overlying soft clay. *Hous Build Natl Res Cent J* 12:71–77. <https://doi.org/10.1016/j.hbrcj.2014.07.004>
61. Kumar A, Ohri ML, Bansal RK (2006) Bearing capacity tests of strip footings on reinforced layered soil. *Geotech Geol Eng* 25:139–150. <https://doi.org/10.1007/s10706-006-0011-6>

**Publisher's Note** Springer Nature remains neutral with regard to jurisdictional claims in published maps and institutional affiliations.